

Hydrothermal Synthesis of Zinc Oxide Crystals in Homogeneous Mixture of Carbon Dioxide, Hydrogen, and Water

Kiwamu Sue,* Kazuhito Kimura, Kenji Murata, and Kunio Arai

Graduate School of Environmental Studies, Tohoku University, Aramaki-aza-aoba 07, Aoba-ku, Sendai 980-8579

(Received March 18, 2004; CL-040310)

Hydrothermal synthesis of zinc oxide crystals in supercritical formic acid (FA) solutions was carried out at 400 °C. Increasing FA concentration from 0.0 to 1.0 mol·kg⁻¹ gave hexagonal plates, hexagonal pillars, and tube-like shapes. Depending on FA concentration, relative intensity of emission spectra at around 500 nm increased from 0.53 to 1.0, peak at 388 nm shifted to 393 nm, and atomic ratio O/(O + Zn) decreased from 49 to 38%.

Zinc oxide (ZnO) has attracted much interest in applications such as short-length light-emitting, transparent conductors, piezoelectric materials, and room temperature ultraviolet lasing.¹ Further, it is widely known that doping of metal cations and inorganic gases like nitrogen and hydrogen changes the intensity of emission spectra and the band gap of ZnO.² Many researchers have proposed synthesis methods for ZnO compounds.¹ Among them, hydrothermal synthesis is one of the most promising techniques for producing crystals from single nano to millimeter size.³

Over the latest decade, we have carried out hydrothermal syntheses of metal oxide particles at supercritical water conditions.³ Water of its supercritical state forms homogeneous mixtures with gases and has specific physical properties that can be controlled with temperature and pressure such as the dielectric constant and ion product.⁴ This means that particle size, morphology, composition, and crystal structure can possibly be varied with temperature and pressure. For the case of redox reaction, concentration of oxygen and hydrogen can be used in homogeneous reaction environments.³ Generally, near the critical pressure of water ($P_C = 22.1$ MPa), the reaction rate of hydrothermal synthesis above water's critical temperature ($T_C = 374$ °C) is a few orders of magnitude higher than that below T_C .³ This, along with the highly variable metal oxide solubility above T_C , provides an excellent environment for forming nano to millimeter size crystals. Recently, use of homogeneous mixture of supercritical water and carbon dioxide was reported as a mild acid catalyst for dehydration reaction of organics.⁵ This technique has also large potential for controlling metal oxide solubility and related solution environments in the field of metal oxide synthesis.

In this study, we report first attempt of hydrothermal synthesis of ZnO using carbon dioxide as a mild acid catalyst for de-

creasing solution pH (increasing metal oxide solubility) and hydrogen as an in situ doping agent in homogeneous reaction field of carbon dioxide, hydrogen, and water.

Solutions were prepared by dissolving precise amount of zinc acetate ($Zn(CH_3COO)_2$, Wako Pure Chemicals, Osaka, Japan) in distilled water and formic acid (HCOOH) standard solution (Wako Pure Chemicals, Osaka, Japan). The concentration of zinc acetate was 0.05 mol·kg⁻¹ and that of formic acid changes from 0.0 to 1.0 mol·kg⁻¹.

Zinc acetate and formic acid aqueous solutions were loaded into a 153-cm³ batch reactor made of Ti alloy. The temperature was measured with a K-type thermocouple that was inserted into the reactor. Reactor load water density was 0.35 g·cm⁻³, which corresponds to about 30 MPa at a reaction temperature of 400 °C. The reactor was heated by immersion into a temperature-controlled molten-salt bath. Approximately 5 min was required for the batch reactor to reach the reaction temperature. Reaction time was 10 min, which includes heating up time. The reactor was quenched in a water bath, which was kept at room temperature.

In this study, hydrothermal reaction is represented in terms of two reaction steps; zinc hydroxide formation and dehydration from the hydroxide. Formic acid decomposes into hydrogen and carbon dioxide and yields of H₂ and CO₂ increase to ca. 90% at 400 °C within 2 s.⁶

The crystal structures of the products were analyzed by powder X-ray diffractometry (XRD) (RINT 2200VK/PC, Rigaku), using Cu K α radiation. The emission spectra of the products were measured by a fluorescence spectrophotometer (F-4500, HITACHI). The wavelength range for these spectra was from 370 to 700 nm and the used excitation wavelength was 378 nm. Observation of these products was performed by scanning electron microscope (SEM) (LEO 1420-OMEGA, Karl Zeiss). Compositions of Zn and O in ZnO crystals were determined by energy-dispersive X-ray spectroscopy (EDS) (JED-2200, JOEL). The concentrations of remaining Zn ion in the recovered aqueous solution were measured by inductively coupled plasma (ICP) emission spectroscopy (SPS-7800, Seiko). Conversion of Zn ion to solid product was defined as $(1 - C/C_0) \times 100$, where C and C_0 are molal concentrations of the Zn species in the recovered and starting solutions, respectively.

SEM images of synthesized crystals are shown in Figure 1. All peaks of these crystals were assigned to zinc oxide as shown

Table 1. Summary of analytical results of zinc oxide crystals at given HCOOH concentrations

HCOOH /mol·kg ⁻¹	Relative Intensity of Peak (500 nm)/—	Peak Position /nm	Conversion /%	O/(Zn + O) /atomic %
0.00	0.53	388	28.2	49
0.25	0.63	390	47.9	42
0.50	1.00	393	66.6	37
1.00	0.80	392	56.9	38

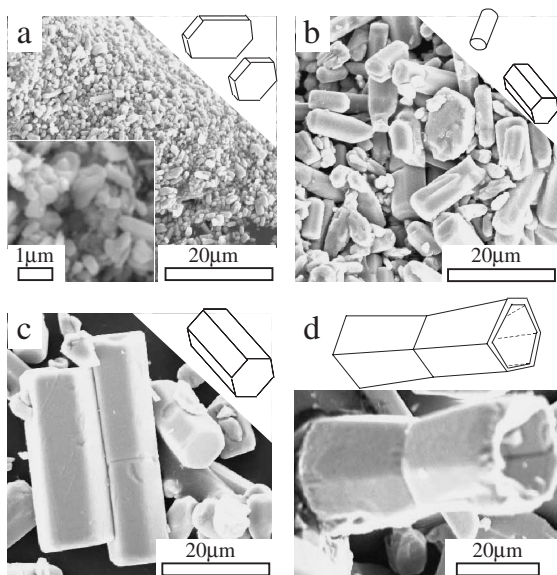


Figure 1. SEM images of ZnO crystals: (a) without FA, (b) $0.25 \text{ mol}\cdot\text{kg}^{-1}$ FA, (c) $0.5 \text{ mol}\cdot\text{kg}^{-1}$ FA, (d) $1.0 \text{ mol}\cdot\text{kg}^{-1}$ FA.

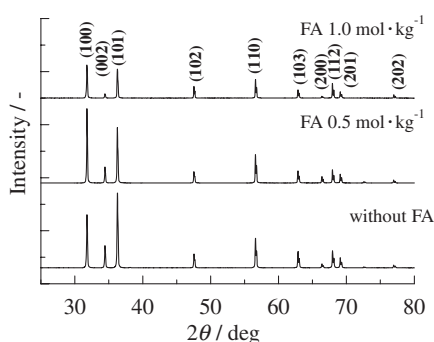


Figure 2. XRD patterns of ZnO crystals.

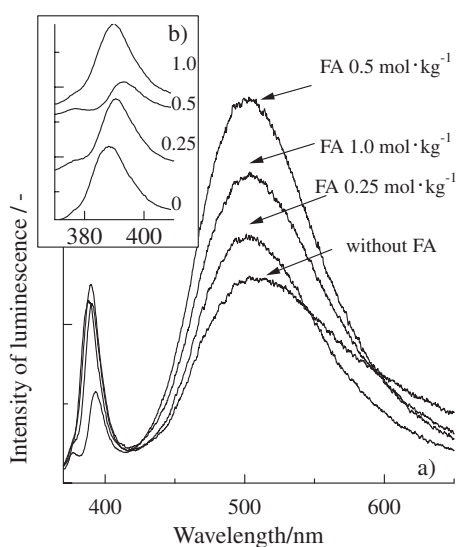


Figure 3. Emission spectra of ZnO crystals.

in Figure 2. The emission spectra of the obtained ZnO crystals are shown in Figure 3. Atomic ratio, $O/(Zn + O)$, and conversion are summarized in Table 1 with the results of emission spectra measurement and conversions.

Main crystal shape was hexagonal plate without FA (Figure 1a), hexagonal pillar and column at $0.25 \text{ mol}/\text{kg}$ FA (Figure 1b), larger hexagonal pillar at $0.5 \text{ mol}/\text{kg}$ FA (Figure 1c), and tube-like hexagonal pillar at $1.0 \text{ mol}/\text{kg}$ FA (Figure 1d). With increasing FA concentration up to $0.5 \text{ mol}/\text{kg}$, the thickness of hexagonal plate increased sharply from ca. $0.1 \mu\text{m}$ to ca. $30 \mu\text{m}$ that is hexagonal pillar (Figure 1c). Then increasing FA concentration up to $0.5 \text{ mol}/\text{kg}$, conversion and intensity of emission spectra increased and atomic ratio of $O/(Zn + O)$ decreased. The peak around 390 nm shifted to longer wavelength side as shown in Figure 3b) (inset).

In general, the emission spectrum of ZnO has two peaks at around 390 and 500 nm as shown in Figure 3.^{7,8} First peak at UV region is assigned to the recombination of excitonic centers.⁷ Many researchers reported the doping of metal cations or inorganic atoms shifted this peak position.⁷ Second peak at visible region is originated from the optical recombination at defect in the crystal, such as oxygen vacancies.⁸ Therefore, we assumed that the shift of first peak was resulted by hydrogen doping into ZnO crystal structure. Further, the doping also decreased atomic ratio $O/(O + Zn)$ and as a result the intensity of second peak increased. The increase of FA concentration decreases pH and increases ZnO solubility. This also means the decreasing nucleation rate for decreasing degree of supersaturation. As a result larger crystals were produced. Then, XRD peaks shown in Figure 2 are different between crystals with and without FA. The addition of FA changed the distribution of dissolved chemical species and it probably changed the growth rate on each surface. However, at present, it is difficult to explain the growth mechanism of the crystals as shown in Figure 1 by traditional crystal growth mechanism.⁹

In conclusions, uses of carbon dioxide as a mild acid catalyst at supercritical condition and supercritical water–hydrogen homogeneous field for a in situ doping of gases can be expected as an attracting field for production of new functional metal oxide crystals.

This research was partially supported by the Ministry of Education, Culture, Sports, Science and Technology, Grant-in-Aid for Scientific Research, No. 15360416.

References

- 1 S. J. Pearton, D. P. Norton, K. Ip, Y. W. Heo, and T. Steiner, *Superlattices Microstruct.*, in press.
- 2 N. Ohashi, T. Ishigaki, N. Okada, T. Sekiguchi, I. Sakaguchi, and H. Haneda, *Appl. Phys. Lett.*, **80**, 1869 (2002).
- 3 a) T. Adschiri, Y. Hakuta, K. Sue, and K. Arai, *J. Nanopart. Res.*, **3**, 227 (2001). b) K. Sue, K. Murata, K. Kimura, and K. Arai, *Green Chem.*, **5**, 659 (2003). c) K. Sue, K. Kimura, K. Murata, and K. Arai, *J. Supercrit. Fluids*, in press.
- 4 a) J. S. Gallagher, R. Crovetto, and J. M. H. L. Sengers, *J. Phys. Chem. Ref. Data*, **22**, 431 (1993). b) T. M. Seward and E. U. Franck, *Ber. Bunsen-Ges. Phys. Chem.*, **85**, 2 (1981).
- 5 K. Minami, T. Sato, K. Sue, and K. Arai, *Catal. Commun.*, submitted.
- 6 J. Yu and P. E. Savage, *Ind. Eng. Chem. Res.*, **37**, 2 (1998).
- 7 M. H. Huang, Y. Wu, H. Feick, N. Tran, E. Weber, and P. Yang, *Adv. Mater.*, **13**, 113 (2001).
- 8 K. Vanheusden, W. L. Warren, C. H. Seager, D. R. Tallant, and J. A. Voigt, and B. E. Gnade, *J. Appl. Phys.*, **79**, 7983 (1996).
- 9 W. Li, E. Shi, W. Zhong, and Z. Yin, *J. Cryst. Growth*, **203**, 186 (1999).